

Stacked Nanosheet Gate-All-Around Transistor to Enable Scaling Beyond FinFET

N. Loubet¹, T. Hook¹, P. Montanini¹, C.-W. Yeung¹, S. Kanakasabapathy¹, M. Guillorn¹, T. Yamashita¹, J. Zhang¹, X. Miao¹, J. Wang¹, A. Young¹, R. Chao¹, M. Kang², Z. Liu¹, S. Fan¹, B. Hamieh¹, S. Siegel¹, Y. Mignot¹, W. Xu¹, S.-C. Seo¹, J. Yoo², S. Mochizuki¹, M. Sankarapandian¹, O. Kwon², A. Carr¹, A. Greene¹, Y. Park², J. Frougier³, R. Galatage³, R. Bao¹, J. Shearer¹, R. Conti¹, H. Song², D. Lee², D. Kong¹, Y. Xu¹, A. Arceo¹, Z. Bi¹, P. Xu¹, R. Muthinti¹, J. Li¹, R. Wong¹, D. Brown³, P. Oldiges¹, R. Robison¹, J. Arnold¹, N. Felix¹, S. Skordas¹, J. Gaudiello¹, T. Standaert¹, H. Jagannathan¹, D. Corliss¹, M.-H. Na¹, A. Knorr³, T. Wu¹, D. Gupta¹, S. Lian², R. Divakaruni¹, T. Gow¹, C. Labelle³, S. Lee², V. Paruchuri¹, H. Bu¹, and M. Khare¹

IBM Research, 257 Fuller Road, Albany, NY 12203

¹IBM, ²Samsung Electronics, ³GLOBALFOUNDRIES, email: njloubet@us.ibm.com

Abstract

In this paper, for the first time we demonstrate that horizontally stacked gate-all-around (GAA) Nanosheet structure is a good candidate for the replacement of FinFET at the 5nm technology node and beyond. It offers increased W_{eff} per active footprint and better performance compared to FinFET, and with a less complex patterning strategy, leveraging EUV lithography. Good electrostatics are reported at $L_g=12\text{nm}$ and aggressive 44/48nm CPP (Contacted Poly Pitch) ground rules. We demonstrate work function metal (WFM) replacement and multiple threshold voltages, compatible with aggressive sheet to sheet spacing for wide stacked sheets. Stiction of sheets in long-channel devices is eliminated. Dielectric isolation is shown on standard bulk substrate for sub-sheet leakage control. Wrap-around contact (WAC) is evaluated for extrinsic resistance reduction. **Keywords:** VLSI, Gate-All-Around, Nanosheet, FinFET.

Introduction

Horizontally stacked GAA Nanowire/Nanosheet structures can answer logic device needs at 5nm technology nodes and beyond. They offer excellent electrostatics and short channel control [1-4], can be fabricated with minimal deviation from FinFET, and circumvent some of the patterning challenges associated with scaled technologies. In the following, we will show the versatility of this technology in term of design, and the significant boost in performance with a better $W_{\text{eff}}/C_{\text{eff}}$ trade off and electrostatics than FinFET for the same footprint. CMOS integration and DC performance of stacked GAA Nanosheets in sub-7nm ground rules will be presented. We will show nFET/pFET devices at aggressive 12nm gate length with good electrostatics, featuring inner spacer and extremely thin silicon channel. Multiple threshold voltage by WFM patterning, dielectric isolation and WAC are evaluated.

Stacked Nanosheet Device Design for sub-7nm

Figure 1 illustrates area scaling by technology node [5-8]. GAA Nanosheet devices are evaluated at the 7nm ground rule [9] as a replacement of FinFET device architecture to enable further scaling down to the 5nm and 3nm nodes. The scaling benefits of using double and single stack Nanosheet structures is illustrated in Fig. 2. With a relaxed pitch, it is possible to match the effective width (W_{eff}) of aggressively scaled FinFETs and even get a 30% increase in W_{eff} when wide Nanosheets are used. The maximum gain in W_{eff} is obtained for the same footprint with a Nanosheet single stack. As shown in Fig. 3, extremely scaled FinFETs fall on the same curve as two stacks of Nanosheet structures with three sheets, as both are limited by the space between the active regions. A better paradigm is a single wide Nanosheet stack as the structure is defined across the entire active footprint, provided that wide sheets can be successfully fabricated as we show here. In our simulations and experiments, we consider stacked Nanosheets with three layers of 5nm sheet thickness and 10nm vertical sheet to sheet spacing. Some examples of optimized inverter and SRAM layouts using single stack Nanosheet structures with sheet widths from 15nm to 45nm are in Fig. 4, showing the opportunities for power/performance tuning in a given cell design, and cell height reduction using an optimized single Nanosheet stack. In term of AC performance, the relative speed of FinFET, stacked Nanowire and stacked Nanosheet are compared in Figs. 5 and 6. It is shown that single stack Nanosheet has superior intrinsic performance for any sheet width compared to FinFET or stacked Nanowires. This is due to reduced parasitic capacitance for a given active width, resulting a better $C_{\text{eff-to-}}/I_{\text{eff}}$ relationship. Nanosheets also have more effective width in a given footprint, and therefore superior capability in driving a capacitive load. Additionally, the continuously variable sheet width, enabled by EUV single exposure, provides for fine-tuning of the necessary width to optimize power/performance on a product design. In contrast, FinFET and stacked Nanowire offer only crude granularity of one or two fins/stacks. Another specific feature of stacked Nanosheet devices is the inner spacer that functions as the effective device spacer for self-aligned junction formation [10]. This module is described in Fig. 7, and shows

optimization of the inner spacer thickness at 5nm with no degradation of the $I_{\text{eff}}/C_{\text{eff}}$ electrical performance.

44/48nm CPP Device Fabrication & Characteristics

With respect to the process flow, it has only a few divergences compared to FinFET technologies. A simplified flow is reported in Fig. 8 with selected cross section TEM from critical steps. The specific elements compared to FinFET are: 1) multilayer channel epitaxy to form stacked sheets, 2) inner spacer formation 3) channel release and 4) multi-threshold voltage processing. Stacked Nanosheet channel release is performed after dummy gate removal in the standard replacement gate integration, using vapor phase HCl [11]. Regarding the multilayer channel epitaxy, we verified that all Si and SiGe layers were pseudomorphic with respect to Si and defect-free (Fig. 9), thanks to optimized surface preparation and epitaxy. In addition, a low thermal budget (<900°C) was employed for shallow trench isolation (STI) formation, limiting Ge diffusion during the fabrication steps (Fig. 10). Id/Vg characteristics for three-sheet nFET and pFET devices reported in Fig. 11a show good electrostatics for an aggressive $L_g=12\text{nm}$ at 44nm CPP with ultra-thin 5nm Si channel. The best electrostatics at 44nm CPP for nFET are $SS_{\text{at}}=75\text{mV/dec.}$ with $DIBL=32\text{mV}$, and for pFET $SS_{\text{at}}=85\text{mV/dec.}$ with $DIBL=24\text{mV}$. A TEM micrograph of the final structure is in Fig. 11b, showing good uniformity in L_{gate} , inner spacer thickness, and epitaxy formation throughout the stack.

Multi-Vt, Long Channel & Performance Improvement

The deformation or bending of the sheets can be of great concern especially for long channel when the sheets are suspended across long distances after channel release. Stiction between Nanosheets can be suppressed with optimized interface layer (IL) dielectric formation; devices with $L_g=150\text{nm}$ show no observable bending or stiction in the TEM cross-section (Fig. 12). As shown in Fig. 13, replacement of P-metal with N-metal for multiple threshold voltages is also possible, even for structures of width in excess of 40nm; there are no residues or damage visible after P-metal replacement when optimized H_2O_2 -based chemistry is employed; this was electrically verified by comparing the threshold voltage of devices with and without the removal process. Figure 14 reports nFET Vt modulation with respect to N-metal WFM thickness, showing a sensitivity in the range 13-14mV/Å, suitable for multi-Vt solutions. The benefits of dielectric isolation are particularly important for Nanosheets on bulk substrates, as shown in Fig. 15. An additional 8% performance improvement is also expected using conformal silicide in a wrap-around contact configuration as described in Fig. 16 [12, results from IBM/Applied Materials].

Conclusion

For the first time, we fabricated and characterized horizontally stacked Nanosheet devices with $L_g=12\text{nm}$ and aggressive 44/48nm CPP. We showed that stacked Nanosheet offers versatile design options for performance and power management thanks to the benefits of large W_{eff} . It has superior electrostatics and dynamic performance compared to extremely scaled FinFETs with multiple threshold and isolation solutions inherited from FinFET technologies. All these advantages make stacked Nanosheet devices an attractive solution as a replacement of FinFETs, scalable to the 5nm device node and beyond, and with less complexity in the patterning strategy.

Acknowledgements: This work was performed by the Research Alliance teams at various IBM Research and Development Facilities. We want to thank for their executive support: T.C. Chen, D.W. Kim, M. Rodder, and G. Gomba.

References: [1] S. Bangsaruntip et al, IEDM, p.1-4, 2009 [2] I. Lauer et al., VLSI, p.140-141, 2015 [3] S.D. Kim et al., S3S Conference, p. 1-3, 2015 [4] H. Mertens et al., IEDM, p.19-7, 2016 [5] C. Auth, et al, VLSI, p.131-133, 2012 [6] S. Wu, et al., IEDM, p. 254-257, 2013 [7] "Intel 14nm Technology", Intel.com, 2014 [8] K. Seo et al., VLSI, p.14-15, 2014 [9] R. Xie et al., IEDM, p. 2-7, 2016 [10] S. Barraud et al., IEDM, p.17-6, 2016 [11] N. Loubet et al., Thin Solid Films, 517(1), p.93-97 [12] N. Breil, A.Carr et al., accepted VLSI 2017.

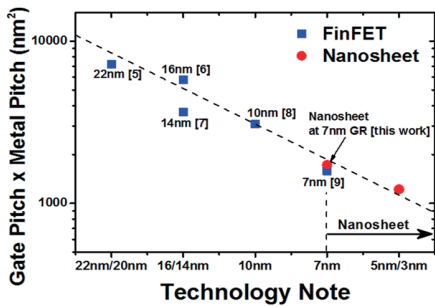


Fig. 1: GAA Nanosheet structures can be a replacement of existing FinFET in sub 7-nm ground rule.

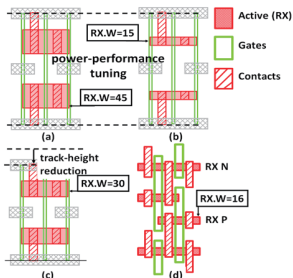


Fig. 4: For a given cell height, the Nanosheet (RX) width can be varied to optimize power-performance trade-offs in logic (a-c) and SRAM (d).

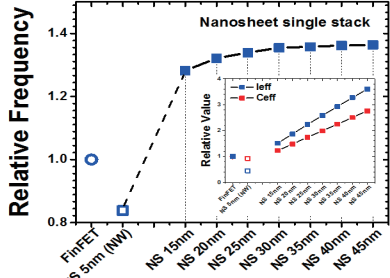


Fig. 5: Relative Frequency for several device options: FinFET, Nanosheet 5nm (Nanowire), and various widths single stack Nanosheets. Inset: C_{eff} and I_{eff} for same devices.

- NS stack epitaxy (a)
- NS "Fin" patterning & STI (b)
- NS "Fin" reveal (c)
- Dummy Gate patterning (d)
- Spacer & Inner Spacer (e)
- Dual SD Epitaxy (f)
- Channel Release (g)
- RMG (h)
- Air Spacer
- Wrap-around contact
- MOL/BEOL (i)

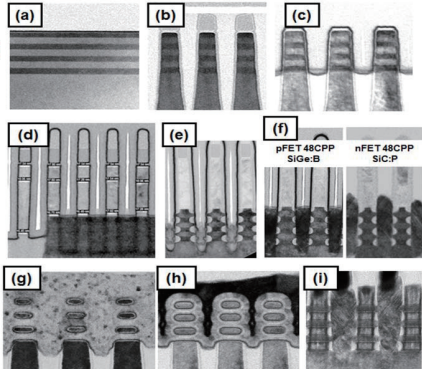


Fig. 8: Stacked Nanosheet Process Sequence & TEM gallery.

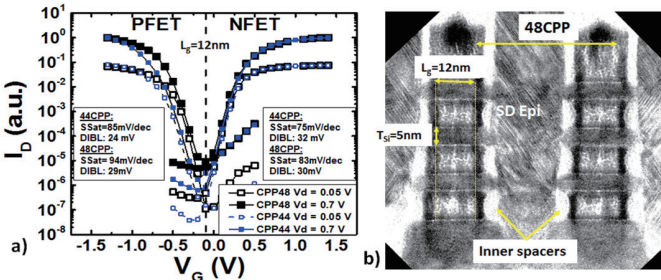


Fig. 11: Stacked Nanosheet 44/48nm CPP nFET/pFET devices I_D/V_G - Structures feature 3 sheets, inner spacer, $L_g=12nm$, and $T_s=5nm$

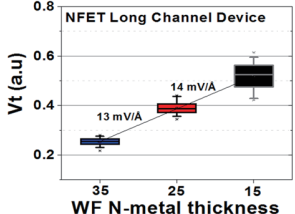


Fig. 14: nFET long channel V_t modulation with N-metal

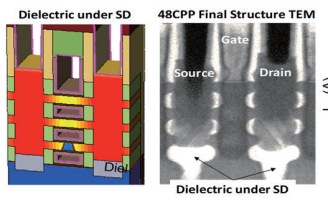


Fig. 15: Sub-sheet leakage suppression when a dielectric is inserted under the source/drain, comparable to fully isolated.

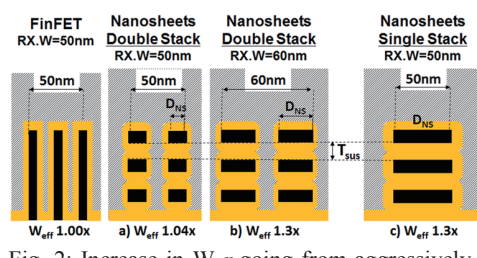


Fig. 2: Increase in W_{eff} going from aggressively scaled FinFET to double and single stack Nanosheets structures. Best improvement is obtained using a single wide Nanosheet stack at constant active width (RX.W).

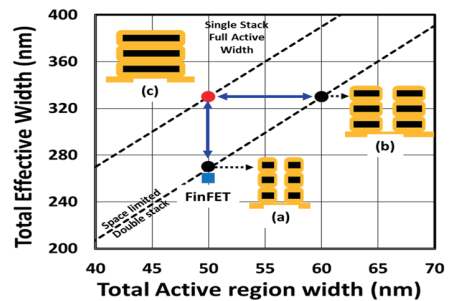


Fig. 3: Improvement in W_{eff} at same footprint going from extremely scaled FinFET to a single wide stack Nanosheet.

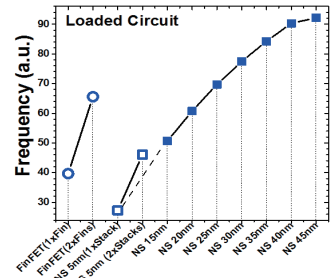


Fig. 6: Inverter driving a capacitive load. Performance of a single wide Nanosheet stack is superior. Note: improved granularity for power optimization.

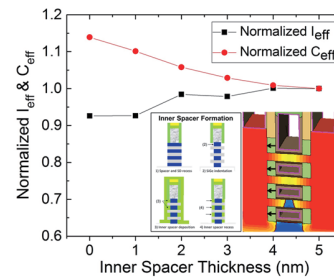


Fig. 7: Normalized I_{eff} & C_{eff} Inner spacer formation is required for integrity of the epitaxy.

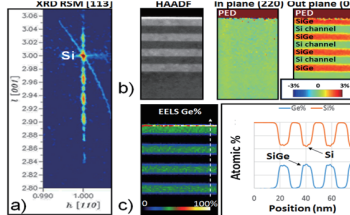


Fig. 9: XRD RSM [113] scan (a), Precession Electron Diffraction (b), and EELS (c) confirm a defect-free pseudomorphic stack

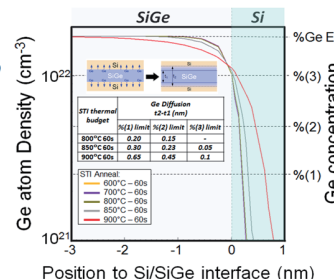


Fig. 10: Ge concentration profiles after different STI anneal temperatures. A small diffusion of Ge is observed at $T < 900^\circ C$

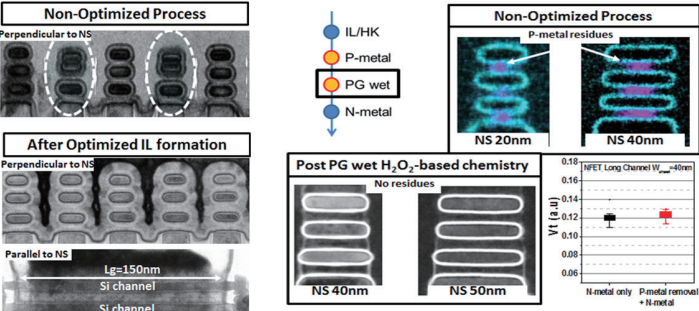


Fig. 12: Stiction between Nanosheets is suppressed with optimized IL formation

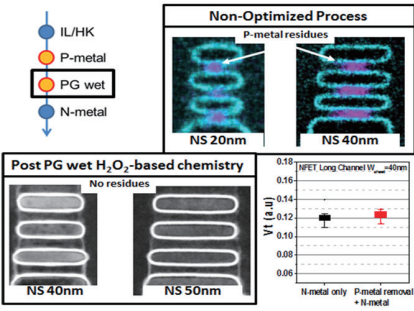


Fig. 13: P-metal can be fully removed in wide Nanosheet structures using H_2O_2 -based chemistry with no impact on the structure and gate stack properties

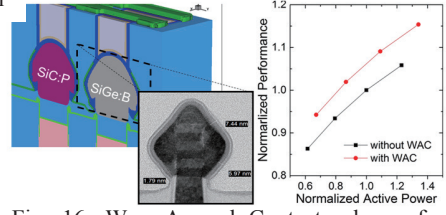


Fig. 16: Wrap-Around Contact scheme for Nanosheet - 8% performance improvement is expected with this technique.